JOURNAL OF SOLID STATE CHEMISTRY 69, 280–288 (1987)

The Iron Electronic Characteristics and the Crystal Dimensionality of the Phases Fe_xTiSe_2 (x = 0.25, 0.38, 0.50)

M. A. BUHANNIC,* P. COLOMBET, AND M. DANOT

Laboratoire de Chimie des Solides, U.A. CNRS n° 279, Université de Nantes, 2, rue de la Houssinière, 44072 Nantes Cédex, France

AND G. CALVARIN

LCPS, U.A. CNRS n° 453, École Centrale, Grande Voie des Vignes, 92290 Chatenay-Malabry, France

Received April 30, 1986; in revised form December 8, 1986

The crystallographically ordered Fe_xTiSe_2 compounds (x = 0.25, 0.38, and 0.50) have been investigated as a function of temperature using Mössbauer spectroscopy, susceptibility measurements, and X-ray diffraction. It is found that the coupling between the iron-d localized and the $TiSe_2$-band levels decreases as x increases, contrary to what is usually observed for lower iron contents in related disordered materials. For x = 0.50, magnetostriction is evidenced below T_N. Besides, the consequences of iron intercalation in $TiSe_2$ are analyzed from the viewpoint of the crystal dimensionality as deduced from a thermal expansion study.

Introduction

In the metallic Fe_xTiSe_2 series with the defect NiAs-type arrangement, the $Fe_{0.50}TiSe_2$ ($FeTi_2Se_4$) compound, with the Cr_3S_4-type structure, was first reported (*1*, *2*) along with some physical properties (*3–6*). A more extensive study of the system as a function of x was then performed (*7*, *8*), which showed the existence of several other phases corresponding to superstructures of the $TiSe_2$ reference cell. The three studied compounds can be schematically described as resulting from a partial occupancy of the Van der Waals gap of $TiSe_2$ by iron. The superstructures occur as a result of an ordering of iron and vacancies in this gap. The cell constants and structural types have already been reported (*7*): $Fe_{0.50}TiSe_2$ belongs to the Cr_3S_4-type structure ($Fe_{0.50}TiSe_2$ = $FeTi_2Se_4$ = M_3X_4), $Fe_{0.38}TiSe_2$ to the $2c'$–Cr_2S_3 type ($Fe_{0.38}TiSe_2$ = $Fe_{0.57}Ti_{1.50}Se_3$ = $M_{2.07}X_3$), and $Fe_{0.25}TiSe_2$ to the M_5X_8 type ($Fe_{0.25}TiSe_2$ = $FeTi_4Se_8$ = M_5X_8) as defined (*9*) by M. Chevreton (M = transition metal; X = S, Se, Te). The corresponding space groups are $I2/m$ (x = 0.50), $P\bar{3}1c$ (x = 0.38), and $F2/m$ (x = 0.25). It should be noticed that the Cr_3S_4 model is quite stable, all the various $FeTi_2Se_4$ samples reported by various authors belonging systematically to this structural type. Furthermore, from a Mössbauer study of $FeTi_2S_4$, it can be thought that, in this structure, the Fe–□ arrangement is nearly perfectly ordered, since the

* To whom correspondence should be addressed.

0022-4596/87 $3.00

spectra can be fitted with only one iron site, even in the magnetic region (*10*). However, slight departures from stoichiometry can possibly induce a tendency to disorder (*10, 11*). As for the two other compositions (x = 0.38 and x = 0.25), there is no evidence that the structures obtained ($2c'$–Cr_2S_3 and M_5X_8) represent the stable states, as different arrangements have been observed by various groups (*7, 8, 12*) without any precise explanation of these differences proposed. Moreover, for the $M_{0.25}TiX_2$ compounds (M = Fe, Co; X = S, Se), single-crystal X-ray crystallographic studies have shown that the M–□ order can be strongly imperfect (*12, 13*).

The magnetic ordering of Fe_xTiSe_2 powder samples ($0 \leq x \leq 0.50$) was recently studied (*14*): for lower iron concentrations ($x < 0.20$), a spin glass state occurs, whereas for higher iron concentrations ($x > 0.20$), an antiferromagnetic behavior is observed. The former behavior is related to (i) the disordered character of the iron-vacancy distribution in the Van der Waals gap and (ii) the RKKY contribution to the coupling between the iron magnetic moments, possibly together with a competition between the superexchange interactions. The latter behavior results from the onset of iron-vacancy ordering when x is greater than 0.20.

However, little is known about the physical properties of the ordered states as a function of the iron content. The present work deals with the properties of three compounds belonging to the Fe_xTiSe_2 system (x = 0.25, 0.38, and 0.50). Mössbauer spectroscopy, accurate X-ray diffraction study, and polycrystalline as well as single-crystal susceptibility measurements have been carried out from 4 to 300 K. The synthetic procedure has been given elsewhere (*7*). As for the physical measurement experimental procedures, they will be presented separately. Owing to the fact that every crystal sample is bound to be twinned, such samples will be hereafter denoted as "crystals" and not "single crystals."

Room-Temperature ^{57}Fe Mössbauer Study

The Mössbauer spectra (Fig. 1) were obtained at 295 K with an ~10-mCi $^{57}Co(Rh)$ source and an "Elscint" spectrometer using a symmetrical sawtooth vibrator. Only polycrystalline samples were studied. Whatever the composition may be, the spectra can be fitted using a quadrupolar doublet. The characteristics of the spectra vary slightly as a function of the composition, as shown in Table I.

The lower Δ value observed for x = 0.38 may possibly be related to the higher symmetry of this compound (trigonal) as compared to the two others which are monoclinic.

The isomer shifts (δ) are all located in the range corresponding to ferrous iron in an

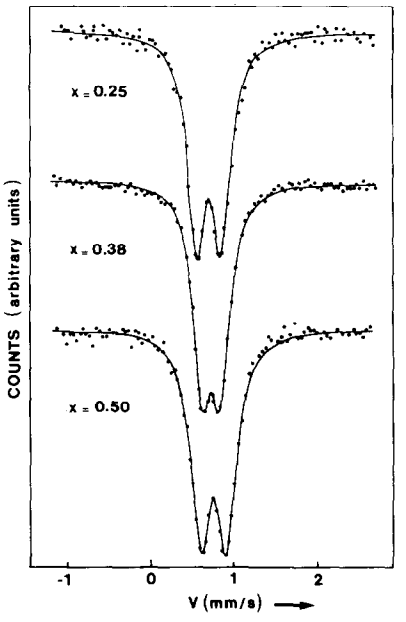

FIG. 1. Room-temperature Mössbauer spectra of Fe_xTiSe_2.

TABLE I

MÖSSBAUER PARAMETERS OF Fe_xTiSe_2 COMPOUNDS AT ROOM TEMPERATURE

x	δ_a ($\pm$0.01 mm sec^{-1})	Δ ($\pm$0.01 mm sec^{-1})	Γ_b ($\pm$0.01 mm sec^{-1})
0.25	0.74	0.31	0.14
0.38	0.77	0.24	0.14
0.50	0.79	0.33	0.15

[a] Relative to α-Fe at 295 K.
[b] Half-width at half-height.

octahedral covalent surrounding (*15*). The δ value increases with x in contrast with what is expected assuming covalency effects only. Effectively, and following the competing bond principle, the Fe–Se bond covalency increases as the iron content increases, as shown in the nonmetallic Fe_xZrX_2 (X = S, Se) compounds (*16*). As a consequence (*17*), δ should decrease from $x = 0.25$ to $x = 0.50$.

However, as far as the M_xTX_2 intercalation compounds are concerned (M and T are transition metals), it is known that the M–3d electrons interact with the conduction electrons. The localized M moments then contribute to the electron scattering in the paramagnetic range (spin–flip scattering). Hence, in the resulting mixed levels, the ionic ones (essentially of M character) become spatially less localized. Simultaneously, a compensating spin polarization of the conduction electrons (essentially of T character) appears. In particular, this effect is drastically reduced below the magnetic ordering temperature. The magnitude of this interaction may thus be estimated from resistivity measurements by considering the spin–disorder resistivity as defined by the difference in the resistivity at $T = O$ extrapolated from above the magnetic transition to that measured at low temperature (*18*). Then, from the data available in the literature, it turns out that the spin–disorder resistivity decreases as the M content increases as far as the crystallographically ordered compounds are concerned (Table II) (*19, 20*).

Consequently, in the studied compounds, the 3d-iron electrons should be more and more localized as x increases. This effect may overcome the effect due to covalency increase, leading to δ values increasing with x, as experimentally observed. Such a behavior is not unique though not hitherto noticed (see the δ value for Fe_xNbS_2 (*21, 22*), Fe_xTaS_2 (*23*), and Fe_xTiS_2 (*24, 25*)). The δ evolution in the metallic ordered iron intercalation compounds is thus dominated by the effect due to the lowering of the Fe- and T-d interactions as x increases, the metallic Fermi level and the virtual ionic 3d levels being further and further apart.

The disordered related compounds ($x < 0.20$) produce an opposite trend. In spite of the increase in the donated electron number, the resistivity of such materials increases when x increases (*14, 18, 26, 27*), which means that the above discussed interaction increases. We hence predict that the δ value will decrease. To our knowledge, no Mössbauer spectroscopy experiment has been done on this topic.

Magnetic Susceptibility Measurements

The change in χ as a function of temperature for crystal as well as polycrystalline samples was determined, from 4 to 300 K, using a Faraday balance system at several fields from 1 to 7.8 kG. Since the studied selenides are slightly sensitive to oxygen and moisture, the samples were transferred

TABLE II

SPIN–DISORDER RESISTIVITY ($\Omega \cdot$ cm) FOR TWO ORDERED INTERCALATION COMPOUNDS

Compound	$x = 0.25$	$x = 0.33$	Reference
Mn_xTaS_2	1.1×10^{-4}	0.6×10^{-4}	(*19*)
Mn_xNbS_2	3.3×10^{-4}	0.4×10^{-4}	(*20*)

to the helium gas-filled apparatus chamber from the sealed silica tubes as rapidly as possible to avoid deterioration. For the $Fe_{0.50}TiSe_2$ polycrystalline sample, the susceptibility varies as a function of the field strength within a few percent. At higher fields, χ was found to vary linearly with H^{-1}, so that the Honda–Owen method could be applied to derive the infinite-field susceptibility. Such a behavior is indicative of the presence of a ferromagnetic impurity which was identified, later on through a neutron diffraction study, as traces of elemental iron. The susceptibilities were corrected for the diamagnetism of the constituents. However, they were not corrected from the Pauli paramagnetism contribution since, in the temperature range of the study, the χ^{-1} vs T curves do not show off any discrepancy from linearity. This means that below 300 K, the Pauli term is much smaller than the term arising from the iron localized moments. The effective moments μ_{eff}, as well as the Weiss constants θ_p ($\chi = C/(T - \theta_p)$), have been calculated in the range 150–300 K, depending on the composition (Table III).

For all compositions, the susceptibility is

TABLE III

THE EFFECTIVE MOMENTS (μ_{eff}) FOR Fe_xTiSe_2 (μ_B) AND THE NÉEL TEMPERATURES (K)

x	0.25	0.38	0.50
μ_{eff}			
$H_\perp c$	4.2	4.2	4.1
$H_\parallel c$	4.2	4.1	3.9
Powder	4.2	4.1	4.0
T_N			
Crystal	62	95	129
Powder	83	55	129
θ_p[a]			
$H_\perp c$	−60	−73	−80
$H_\parallel c$	+ 8	+14	+18
Powder	−23	−39	− 9

[a] θ_p is defined in the text.

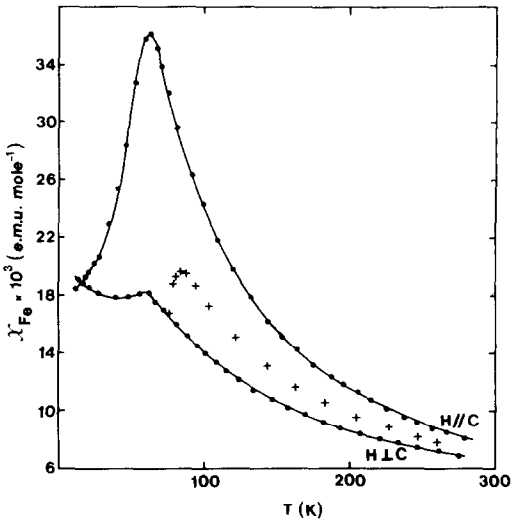

FIG. 2. Magnetic susceptibility as a function of temperature for crystal (●) and polycrystalline (+) samples of $Fe_{0.25}TiSe_2$.

strongly anisotropic in the paramagnetic temperature range, as well as at the lower temperatures (Figs. 2, 3, and 4), as is commonly observed for Fe(II) in an octahedral environment, specifically in the Fe_xTX_2 materials (*5, 14, 19, 27–29*). This is due to strong spin–orbit coupling for the orbitally degenerate ground state of divalent iron (*19*). Moreover, all the compounds are antiferromagnetic, with the easy axis direction close to that of the *c*-axis, i.e., perpendicular to the selenium sheets (Figs. 2, 3, and 4).

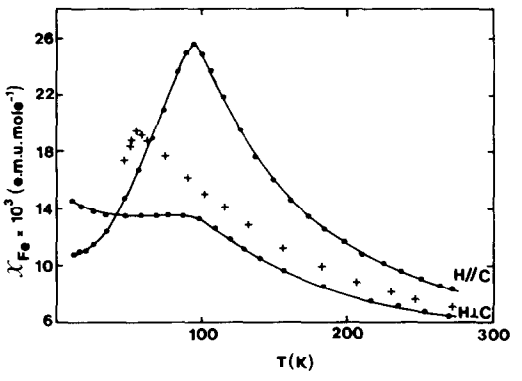

FIG. 3. As in Fig. 2 but for $Fe_{0.38}TiSe_2$.

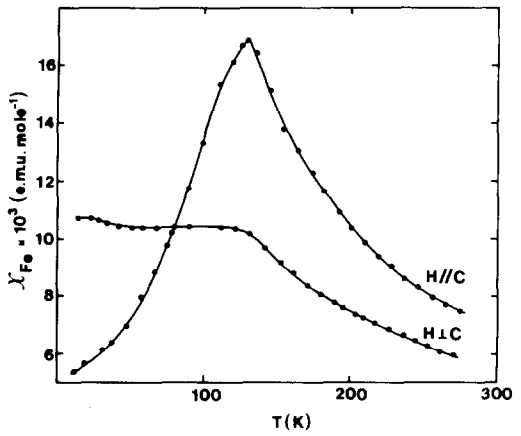

FIG. 4. Magnetic susceptibility as a function of temperature for a crystal sample of $Fe_{0.50}TiSe_2$.

The polycrystalline sample susceptibility is approximately equal to $(\frac{1}{3}\chi_{\parallel} + \frac{2}{3}\chi_{\perp})$ in the temperature range of the study ($x = 0.50$) or, at least, in the paramagnetic region ($x = 0.25$ and 0.38). For $x = 0.50$, the temperature (T_m) where χ is maximum is the same for the powder and for the crystal. Hence the corresponding susceptibility curve for the powder is not shown in this paper. On the contrary, for $x = 0.25$ and $x = 0.38$, the T_m values are markedly different for the polycrystalline samples as compared to the crystal samples (Figs. 2 and 3).

First, it may be seen from Table III that the effective moments are considerably lower than the predicted spin-only value for Fe(II) (4.9 μ_B), as already noticed by other workers concerning the Fe_xTX_2 materials, and thus a fortiori lower than the predicted value when taking into account the spin–orbit coupling effect in the c-axis direction (6.4 μ_B (*19*)). This μ_{eff} reduction, currently observed in such compounds, is usually explained by considering covalency and partial delocalization effects (*4*).

Second, for the crystals, the value of T_m is identical for both directions. Owing to the Ising nature of the spins, this may be taken as evidence of the 3-dimensional character of the magnetic lattice (*30*), despite the fact that the titanium-containing layers can be expected to decouple the magnetic planes. The 3D character is, however, not surprising on the grounds of the significant interactions between the mainly Ti-conduction electrons and the Fe-partially localized moments. As a result (*31*), T_m can be considered as the critical temperature T_N (Table III).

Third, a discrepancy is observed between the values of T_N for crystal and powder samples as far as the $x = 0.25$ and 0.38 materials are concerned. This can be related to the nature of the iron-vacancy ordered arrangement, which may be different for powders and crystals owing to different preparation conditions. Yet, this is not clearly demonstrated by means of the usual diffraction techniques. For the powders, the M_5X_8 ($x = 0.25$) and $2c'$–M_2X_3 ($x = 0.38$) types are unambiguously shown to occur. But, for the crystals, no precise structural determination could be done because of their poor quality (they appear as mosaics in the basal plane). In addition, X-ray diagrams obtained after grinding the crystals do not produce any information about the superstructure type due to important broadening of the lines. However, the T_N values for the $x = 0.25$ and 0.38 crystal samples are well in line with that of the M_3X_4 type $x = 0.50$ sample (Fig. 5). As a result, the two former crystal compounds probably belong to the iron-defect M_3X_4 type.

Low-Temperature ^{57}Fe Mössbauer Study

Mössbauer spectra were recorded down to 4.2 K using an "Oxford Instruments" cryostat, and the temperature was regulated with a precision of ±0.5 K. Even at the lowest temperatures, the hyperfine fields observed on the iron nuclei are very weak (Fig. 6) as already reported for $Fe_{0.50}TiS_2$, which exhibits an ~40 kOe hyperfine field at 4.2 K (*11*). Because of these

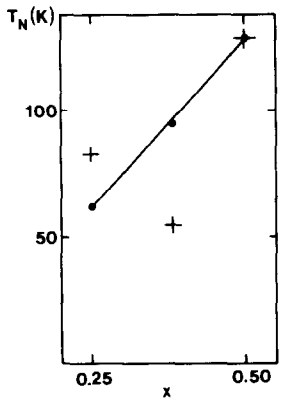

FIG. 5. The Néel temperature, defined as the temperature of the maximum in the χ vs T curve, is plotted as a function of the iron content in the studied Fe_xTiSe_2. (●) Crystals, (+) powders.

low values of H_{hf}, it is quite difficult to determine precisely the magnetic ordering temperatures. For $Fe_{0.50}TiSe_2$, we find T_N = 149 ± 3 K, which is higher than the value derived from the susceptibility curves, as currently observed as a result of short-range magnetic ordering occurrence. For x = 0.38 and 0.25, the magnetic spectra are so narrow that it is nearly impossible to estimate T_N, especially with the poor quality of the present spectra due to the important selenium nonresonant absorption.

Thermal Expansion Measurements

For a lamellar compound, such as TiS_2, the thermal expansion coefficient α_c is twice as large as α_a (a and c representing the hexagonal lattice directions) (*32*). This is the signature of a 2D behavior. To the contrary, for $TiSe_2$, α_a and α_c are reported to be nearly equal above 200 K (18.4 and 19.6 × 10^{-6} K^{-1}, respectively) (*32*), although this compound has a similar structure. α_a is too large and α_c too small. This departure from a 2D behavior (from the viewpoint of the thermal expansion data only), together with the observed α_c singularity at 200 K, has been interpreted (*32, 33*)

TABLE IV

THERMAL EXPANSION COEFFICIENTS (K^{-1})

	$\alpha \times 10^{+6}$				
	α_a	α_b	α_c	α_V	ΔT^a
$TiSe_2$	15.2		16.4	46.8	220–300
$Fe_{0.25}TiSe_2$	13.2	11.6	18.6	43.4	130–300
$Fe_{0.38}TiSe_2$	15.1		19.1	49.3	150–300
$Fe_{0.50}TiSe_2$	13.3	18.1	13.0	44.4	150–300

[a] ΔT indicates the temperature range for which the α's have been calculated.

on the basis of effects due to the occurrence of clusters above 200 K. The same phenomenon occurs for $CrSe_2$ (*34*). These clusters announce the onset of the charge density wave (CDW) state at lower temperatures. From Young's modulus measurements, a thermal expansivity singularity along the a-axis direction was predicted to occur at 200 K (*35*). However, this effect was not observed (*32*).

We did observe it (Fig. 7a) through unit cell thermal expansion measurements performed from 77 to 305 K (±1 K) with the aid of an X-ray device already described (*36*). Our α values (Table IV) are in fair agreement with those reported by Wiegers (*32*) except for the change in the α_a curve

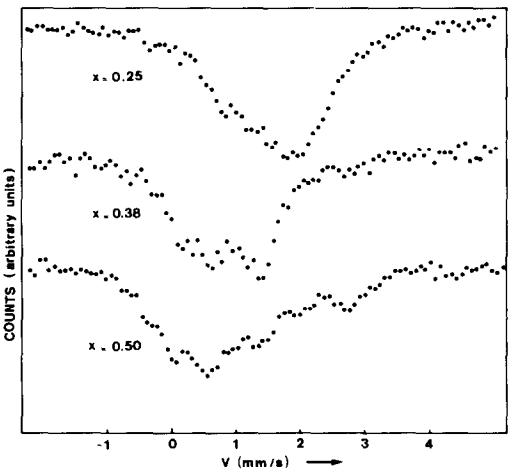

FIG. 6. Fe_xTiSe_2 Mössbauer spectra at 4 K.

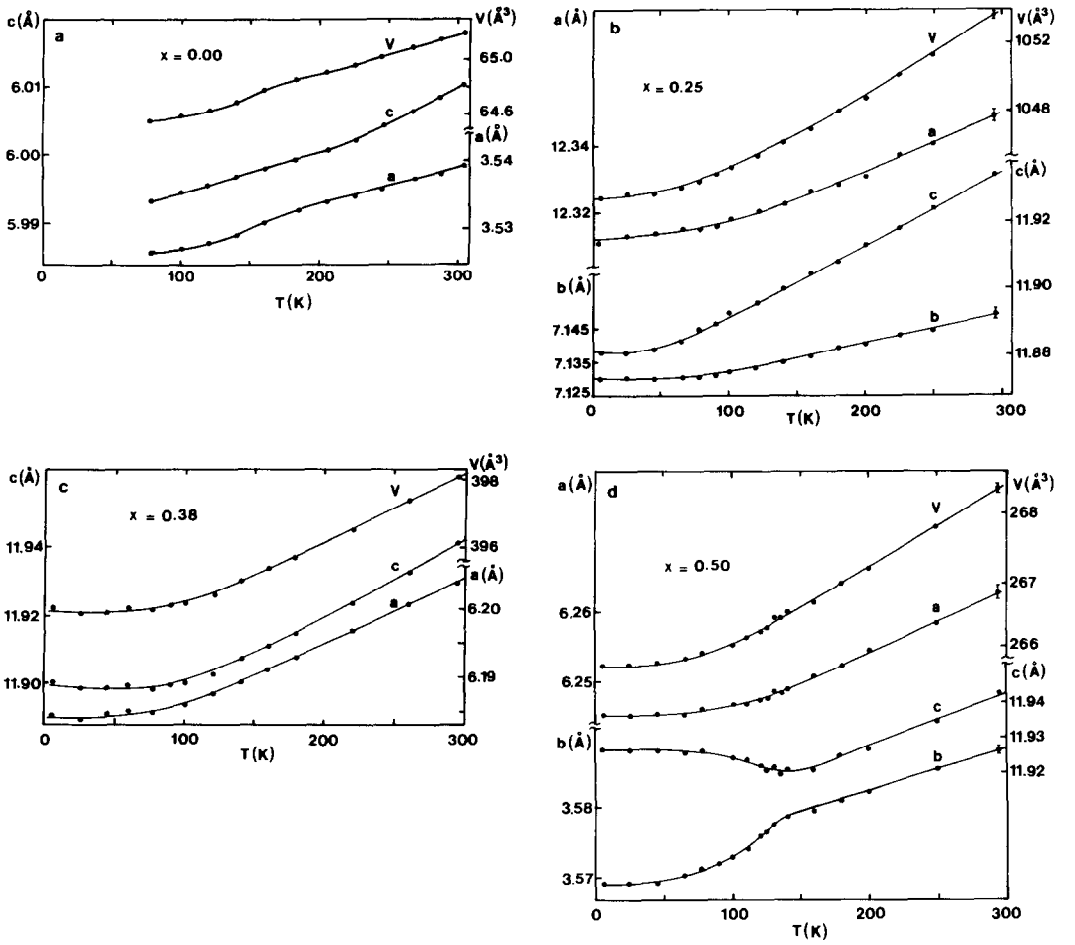

FIG. 7. Thermal evolution of the cell parameters and volume (a, b, c, and V) for crystallographically ordered Fe_xTiSe_2. (a) $x = 0$, (b) $x = 0.25$, (c) $x = 0.38$, (d) $x = 0.50$.

slope at 185 K which we have detected because of accuracy improvement. The α_a slope calculated just below the singularity is found equal to 25×10^{-6} K^{-1}, i.e, 10×10^{-6} K^{-1} larger than the high-temperature slope, in fair agreement with the 16×10^{-6} K^{-1} difference calculated by M. Barmatz *et al.* (*35*). It is also worthy of note that the α_c singularity is observed at significantly higher temperature (215 K). Moreover, below 185 K and down to 4 K, the 2D behavior is not restored as far as the α values are concerned, contrary to what is observed for $CrSe_2$ below the CDW transition as a result of matching of the clusters from one plane to the next (*34*). In $TiSe_2$, the cluster-involved atoms keep drawing closer and closer, so that α_a becomes still greater and α_c still smaller.

For $Fe_{0.25}TiSe_2$ and $Fe_{0.38}TiSe_2$, the 2D expected anisotropy is observed (Figs. 7b and 7c and Table IV): α is greater along the c-axis than perpendicularly ($\alpha_c > \alpha_{a \text{ or } b}$). That means that the CDW state does not appear. This fact is in agreement with what was observed for nonstoichiometric $TiSe_2$: Di Salvo *et al.* (*33*) reported that 0.03 excess Ti is enough for the density of holes,

and the CDW state, to vanish. Hence, assuming each excess Ti to donate four electrons to the bands, and each Fe only two, 0.06 Fe should be necessary for the same result to be reached. Besides, as far as the α values are concerned, $Fe_{0.25}$ and $Fe_{0.38}TiSe_2$ are less anisotropic than TiS_2. This results from the fact that interstitial iron weakens the 2D character and is consistent with the less pronounced anisotropy for $x = 0.38$ as compared to the iron poorer $x = 0.25$ material.

We now discuss the case of $Fe_{0.50}TiSe_2$. The 2D behavior is not observed (Fig. 7d and Table IV): α_a and α_c are equal, and α_b is surprisingly large. In addition, the α_c and α_b curves display a slope change at ~140 K. This value is close to T_N, so that these singularities can be attributed to magnetic ordering effects. Below the transition, the α behavior becomes still more abnormal: α_b increases still further and α_c decreases still further, enough to become negative. Consequently, the unusual α high-temperature values can be regarded as precursory of what will happen below the magnetic transition, just as for $TiSe_2$ as far as the CDW effects are concerned. According to the ideal structural model, magnetic Fe(II) atoms are nearest crystallographic neighbors along the b-axis ($d_{Fe-Fe} = 3.59$ Å at 300 K), but not along the c-axis. Consequently, magnetic effects could induce the singularity occurring in the change of b, whereas the c singularity could be the reflex of elastic compensation, as suggested by the volume variation which is quite similar to what is usually observed in the absence of any transition (Fig. 7d). More specifically, the fact that the b-axis abnormally shortens denotes an attraction between neighboring spins. Thus, the mechanism of the contraction may be thought to be similar to that proposed by Greenwald and Smart (*37*) and discussed by Kanamori regarding a few antiferromagnets (*38*). To wit, the system energy is lowered as a result of the contraction provided that the exchange parameter is magnified as the Fe–Fe distance is decreased. Obviously, the gain in energy is largest when long-range correlations with the spins aligned along a common direction do occur, i.e., below T_N. As the Fe(II)–Fe(II) distance is small along the b-axis, we expect that the magnetic coupling is mainly governed by direct exchange via t_{2g} orbitals overlapping. Then knowing from the Goodenough–Kanamori rules that such a contribution is ferromagnetic and increases with decreasing distance, and consistent with the above-mentioned mechanism, we predict ferromagnetic correlations as far as the Fe moments along the b-direction are concerned. However, the observed elongation perpendicular to the layers could also be supposed to result from spin–orbit coupling effects considering a one-ion model. Probably, this effect has to be taken into account, as in FeO (*39*), since it has the same consequences. But the absence of any elongation at T_N for the other studied materials (for which no long-range Fe arrangement with 3.6-Å Fe–Fe units appears) precludes that this second mechanism is important.

Neutron diffraction studies are in progress with the aim of confirming the ferromagnetic correlations along the b-direction for the $x = 0.50$ samples.

Acknowledgment

The authors are indebted to Dr. O. Gorochov, who allowed one of them to perform the magnetic anisotropy measurements on his balance.

References

1. G. Berodias and M. Chevreton, *C.R. Acad. Sci. Paris C* **261,** 2202 (1965).
2. R. H. Plovnick, M. Vlasse, and A. Wold, *Inorg. Chem.* **7**(1), 127 (1968).
3. R. H. Plovnick, D. S. Perloff, M. Vlasse, and A. Wold, *J. Phys. Chem. Solids* **29,** 1935 (1968).

4. B. L. MORRIS, R. H. PLOVNICK, AND A. WOLD, *Solid State Commun.* **7,** 291 (1969).
5. S. MURANAKA AND T. TAKADA, *Bull. Inst. Chem. Res. Kyoto Univ.* **51**(5) 287 (1973); *J. Solid State Chem.* **14,** 291 (1975).
6. S. MURANAKA, *J. Phys. Soc. Japan* **35,** 616 (1973).
7. Y. ARNAUD, M. CHEVRETON, A. AHOUANDJINOU, M. DANOT, AND J. ROUXEL, *J. Solid State Chem.* **18,** 9 (1976).
8. J. W. LYDING, M. T. RATAJACK, C. R. KANNEWURF, W. H. GOODMAN, AND J. A. IBERS, *J. Phys. Chem. Solids* **43**(7), 599 (1982).
9. M. CHEVRETON, *Bull. Soc. Fr. Minéral. Cristallogr.* **90,** 592 (1967).
10. G. A. FATSEAS, J. L. DORMANN, AND M. DANOT, *J. Phys. Colloq. C6* **37,** 579 (1976).
11. G. A. FATSEAS, J. L. DORMANN, AND M. DANOT, *J. Phys. Colloq. C2* **40,** 367 (1979).
12. M. DANOT AND R. BREC, *Acta Crystallogr., Sect. B* **31,** 1647 (1975).
13. Y. ARNAUD AND M. CHEVRETON, *J. Solid State Chem.* **36,** 151 (1981).
14. D. R. HUNTLEY, M. J., SIENKO, AND K. HIEBL, *J. Solid State Chem.* **52,** 233 (1984).
15. G. A. FATSEAS AND J. B. GOODENOUGH, *J. Solid State Chem.* **33,** 219 (1980).
16. M. A. BUHANNIC, P. COLOMBET, AND M. DANOT, *Nouv. J. Chim.* **9**(7), 519 (1985).
17. J. GOODENOUGH AND G. A. FATSEAS, *J. Solid State Chem.* **41,** 1 (1982).
18. R. H. FRIEND, *Rev. Chim. Miner.* **19,** 467 (1982).
19. S. S. P. PARKIN AND R. H. FRIEND, *Philos. Mag., B* **41,** 65, 95 (1985).
20. A. LEBLANC-SOREAU, J. ROUXEL, M. F. GARDETTE, AND O. GOROCHOV, *Mater. Res. Bull.* **11,** 1061 (1976).
21. O. GOROCHOV, A. LEBLANC-SOREAU, J. ROUXEL, P. IMBERT, AND G. JEHANNO, *Philos. Mag., B* **43**(4), 621 (1981).
22. M. KATADA, K. SATO, Y. HIRASAWA, AND H. SANO, *Radiochem. Radioanal. Lett.* **54**(5), 293 (1982).
23. M. EIBSCHUTZ, S. MAHAJAN, F. J. DI SALVO, G. W. HULL, AND J. V. WASZCZAK, *J. Appl. Phys.* **52**(3), 2098 (1981).
24. M. KATADA AND R. H. HERBER, *J. Solid State Chem.* **33,** 361 (1980).
25. N. I. SHAPIRO, A. S. GOLUB, R. M. BAGIROV, AND R. A. STUKAN, *in* "Proceedings, ICAME, Alma-Ata, USSR, 1983," in press.
26. D. A. WHITNEY, R. M. FLEMING, AND R. V. COLEMAN, *Phys. Rev. B* **15,** 3405 (1976).
27. S. J. HILLENIUS, R. V. COLEMAN, E. R. DOMB, AND D. J. SELLMEYER, *Phys. Rev. B* **19,** 4711 (1978).
28. M. EIBSCHUTZ, F. J. DI SALVO, G. W. HULL, JR., AND S. MAHAJAN, *Appl. Phys. Lett.* **27,** 464 (1975).
29. M. A. BUHANNIC, M. DANOT, P. COLOMBET, P. DORDOR, AND G. FILLION, *Phys. Rev. B* **34,** 7, 4790 (1986).
30. M. E. FISHER, *J. Math. Phys.* **4,** 124 (1963).
31. M. F. SYKES AND M. E. FISHER, *Physica* **28,** 919 (1962).
32. G. A. WIEGERS, *Physica B + C* **99,** 151 (1980).
33. F. J. DI SALVO, D. E. MONCTON, AND J. V. WASZCZAK, *Phys. Rev. B* **14,** 10, 4321 (1976).
34. C. F. VAN BRUGGEN, R. J. HAANGE, G. A. WIEGERS, AND D. K. G. DE BOER, *Physica B +C* **99,** 166 (1980).
35. M. BARMATZ, R. C. FARROW, AND F. J. DI SALVO, *in* "IEE Ultrasonics Symposium Proceedings, 1977," p. 378.
36. J. F. BERAR, G. CALVARIN, AND D. WEIGEL, *J. Appl. Crystallogr.* **13,** 311 (1980).
37. S. GREENWALD AND J. S. SMART, *Nature (London)* **166,** 523 (1950).
38. J. KANAMORI, *in* "Magnetism" (G. T. Rado and H. Suhl, Eds), Vol. 1, p. 186, Academic Press, New York (1963).
39. *Ibid.*, p. 197.